



# ICLR

International Conference On  
Learning Representations



# Advancing Universal Deep Learning for Electronic-Structure Hamiltonian Prediction of Materials

Shi Yin<sup>1\*†</sup>, Zujian Dai<sup>1\*</sup>, Xinyang Pan<sup>2\*</sup>, Lixin He<sup>2,1,3†</sup>

1 Institute of Artificial Intelligence, Hefei Comprehensive National Science Center

2 Laboratory of Quantum Information, University of Science and Technology of China

3 Hefei National Laboratory, University of Science and Technology of China

\*Equal Contributions, † Corresponding Authors

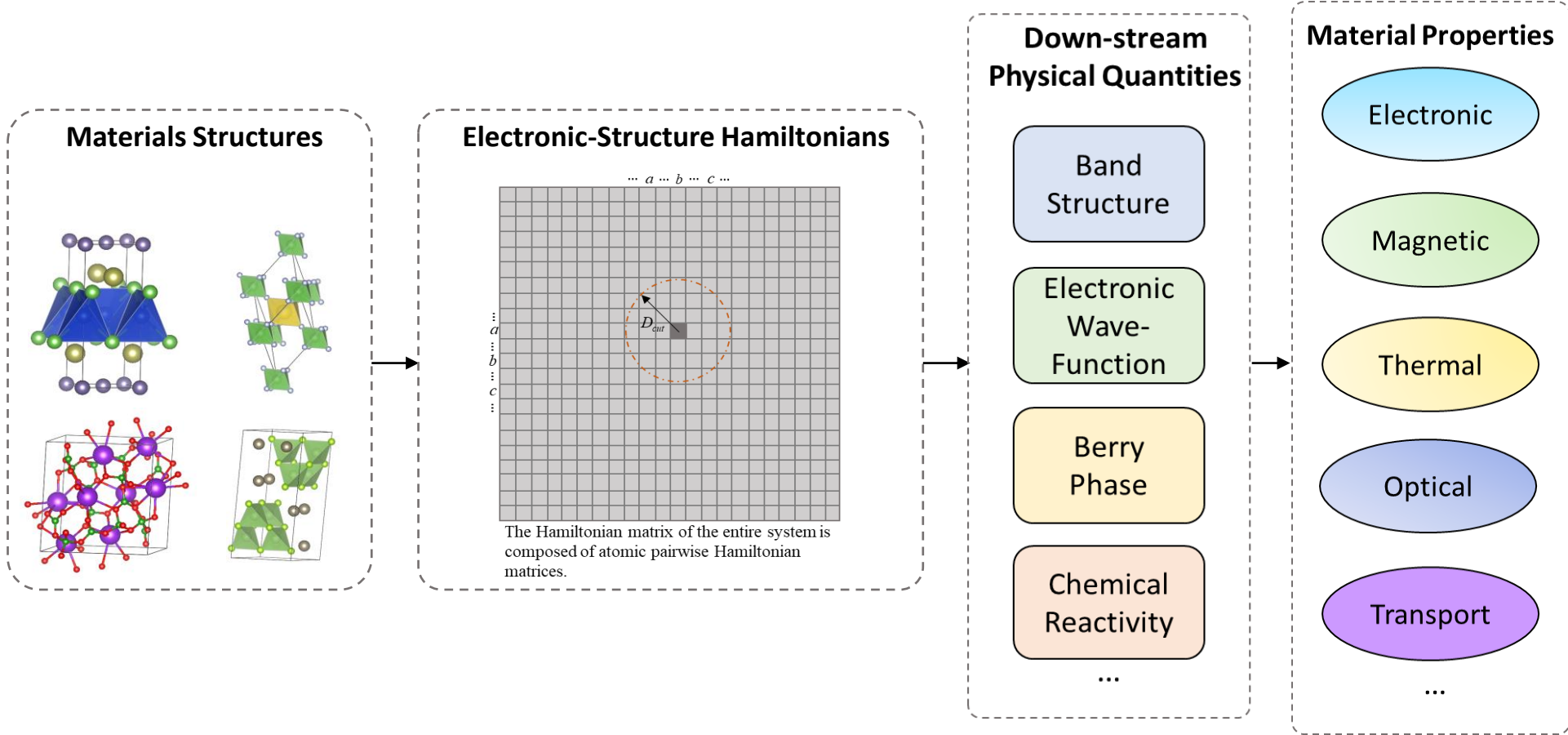
Presenter: Shi Yin

shiyin@iai.ustc.edu.cn

2026.3.30

# • The Central Role of Electronic-Structure Hamiltonians in Materials Science

- **Determining Macroscopic Behaviors:** The Hamiltonian encodes fundamental quantum states (Band Structure, Wave-Function, Berry Phase, etc.), directly bridging to the material's electronic, magnetic, optical, thermal, and transport properties.
- **Enabling Screening:** Fast and accurate Hamiltonian prediction serves as the essential prerequisite for property-driven, large-scale material discovery.



# • Bottleneck of Existing Approaches

## • The Computational Cost of Traditional DFT

- **High Time Complexity (TC):** Extremely expensive Self-Consistent Field (SCF) iterations, scaling at  $O(TN^3)$  (where  $T$  is the number of steps and  $N$  is system size).
- **Scalability Issue:** Prohibitively expensive and practically impossible to scale to large, complex material systems within limited time and computational budgets.

$$TC \sim \begin{cases} O(N^2), & \text{small } N \\ O(N), & \text{large } N \end{cases} \quad TC \sim O(TN^3)$$

$\rho^{(0)}(\mathbf{r}) \rightarrow V_{HXC}^{(0)}[\rho](\mathbf{r}) \rightarrow \mathbf{H}^{(0)} \rightarrow \psi_{nk}^{(0)}(\mathbf{r}) \rightarrow \rho^{(1)}(\mathbf{r}) \rightarrow \dots \rightarrow \rho^{(T)}(\mathbf{r}) \rightarrow V_{HXC}^{(T)}[\rho](\mathbf{r}) \rightarrow \mathbf{H}^{(T)}$

Traditional Density Functional Theory (DFT) methods

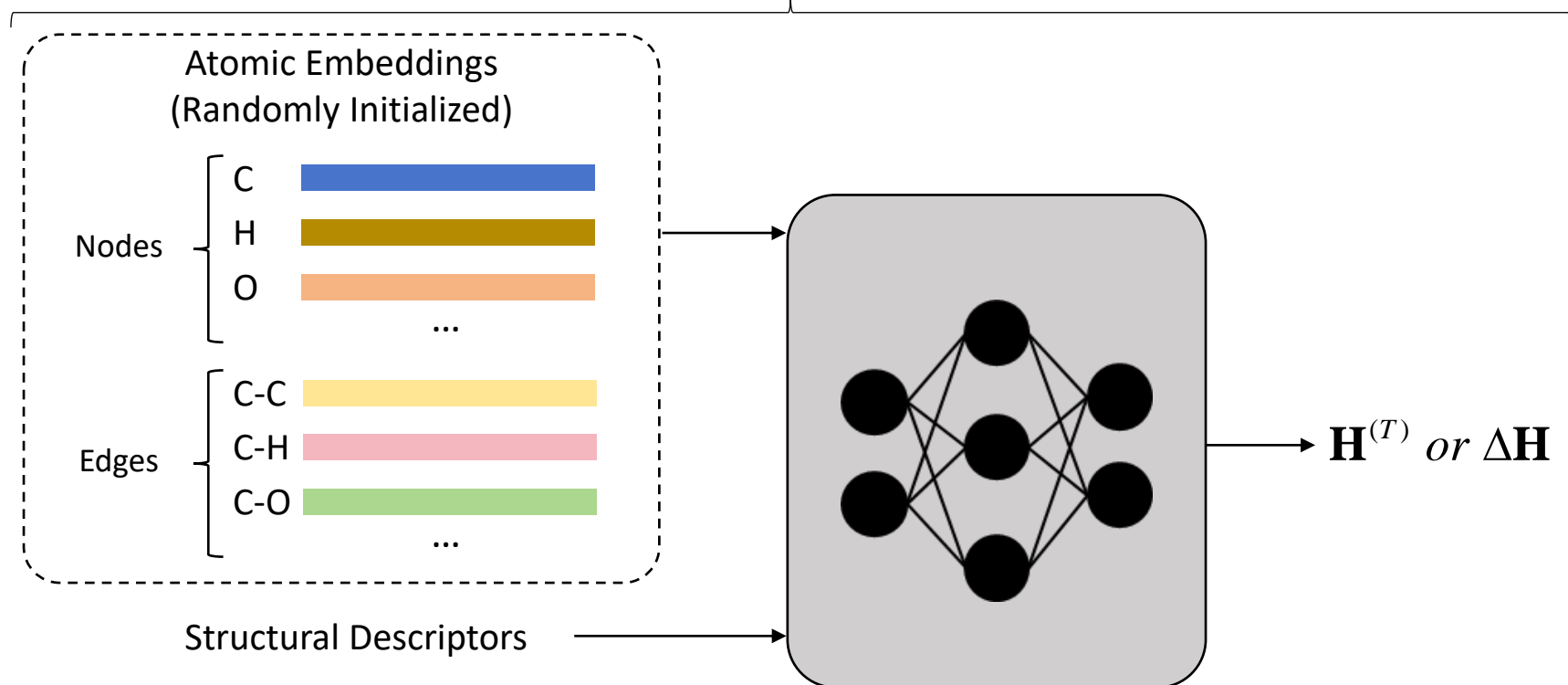
**Huge computational complexity (x)**

# • Bottleneck of Existing Approaches

## • The Generalization Problem of Current Deep Models

- **Lack of Physical Priors:** While successfully bypassing the SCF process for efficiency, current deep models struggle to generalize as universal models across the entire periodic table. Relying on randomly initialized embeddings fails to capture underlying physics, causing poor generalization on rare elements and unseen chemical bonds.

$$TC \sim \begin{cases} O(N^2), & \text{small } N \\ O(N), & \text{large } N \end{cases}$$

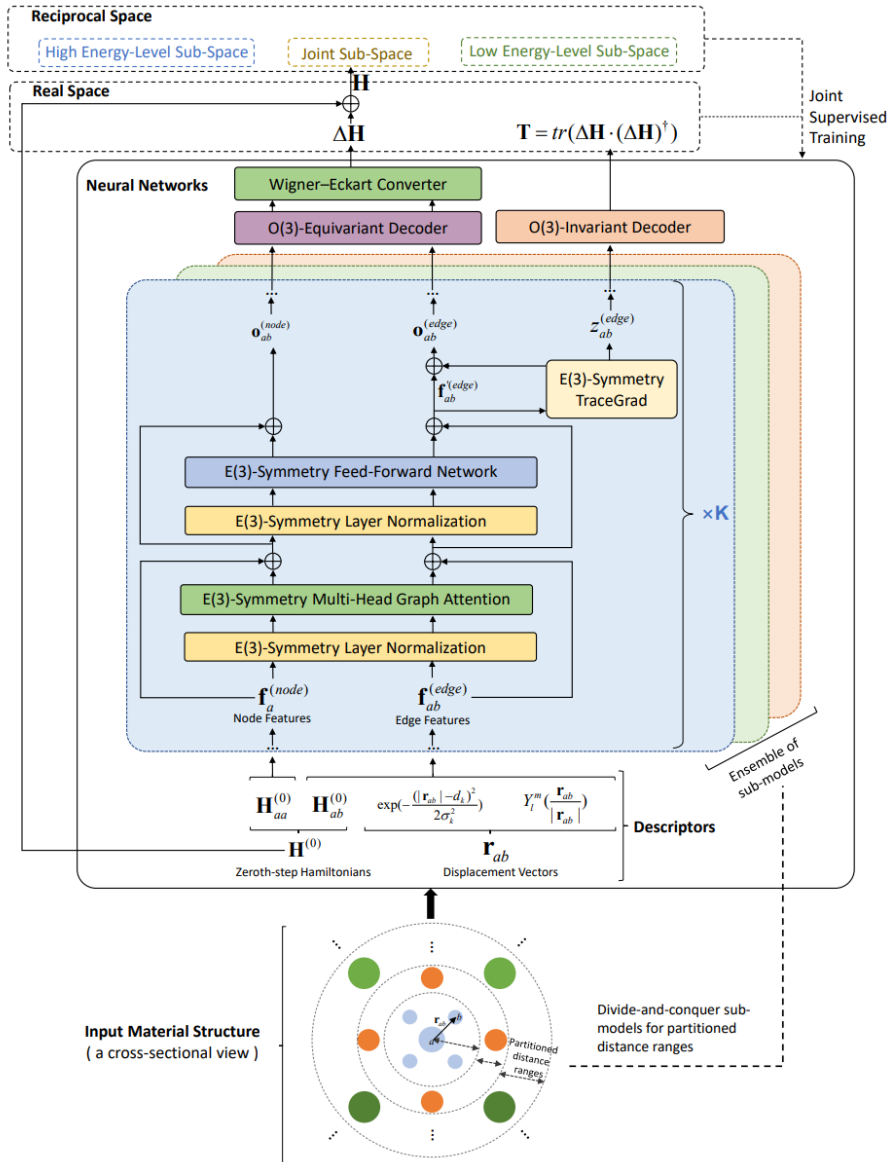


Lightweight  
computational  
complexity ( $\checkmark$ )

The input descriptors  
lack physical priors and  
may suffer from issues  
of sparsity, making it  
difficult for neural  
networks to learn ( $\times$ )

# • Our Approach

## • NextHAM: Advancing Universal Deep Learning for Hamiltonian Prediction



- Physics-Grounded Input Descriptors:** We introduce the zeroth-step Hamiltonians, which can be efficiently constructed by the initial charge density of DFT, as informative input descriptors that enable the model to effectively capture prior knowledge of electronic structures.

- Expressive E(3)-Symmetry Neural Networks:** We present a network architecture that strictly adheres to E(3)-symmetry while maintaining high non-linear expressiveness for Hamiltonian prediction by extending the TraceGrad.

- Joint R-Space & K-Space Loss:** We propose a novel training objective to ensure the accuracy performance of Hamiltonians in both real space and reciprocal space, preventing error amplification and the occurrence of "ghost states" caused by the large condition number of the overlap matrix.

Lightweight computational Complexity ( $\checkmark$ )

Expressive input descriptors, enabling more precise and granular learning performance ( $\checkmark$ )

Advanced network architecture and training objectives ( $\checkmark$ )

# • Our Dataset

- **Materials-HAM-SOC: containing 17,000 material, spanning more than 60 elements from the first six rows of the periodic table and explicitly incorporates spin-orbit coupling (SOC) effects.**

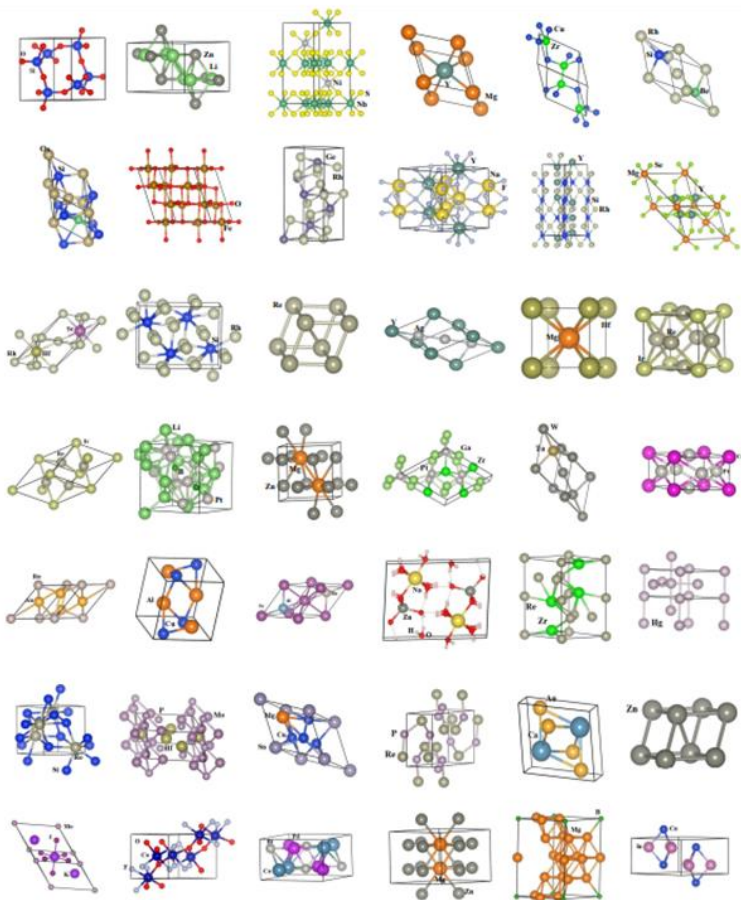


Figure 7: Representative crystal structures sampled from the **Materials-HAM-SOC** dataset. The examples cover diverse chemical compositions, structural patterns, and atomic configurations, demonstrating the dataset's broad coverage across the periodic table. Such diversity ensures that the benchmark provides a comprehensive foundation for training and evaluating universal Hamiltonian prediction models.

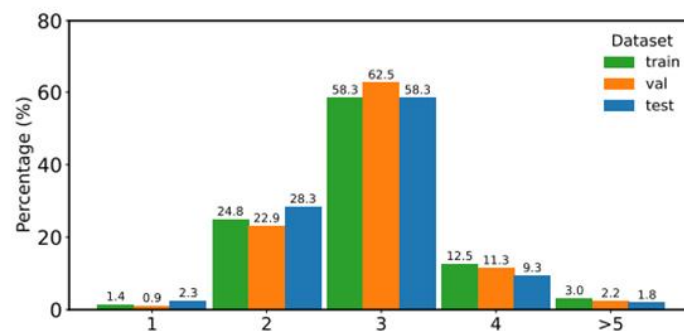


Figure 4: Bar charts of elemental species distributions in the training, validation, and test sets.

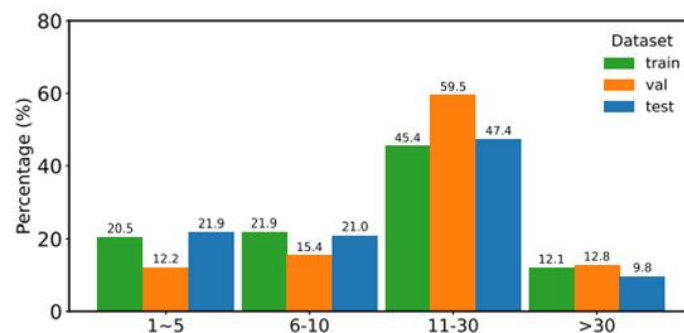
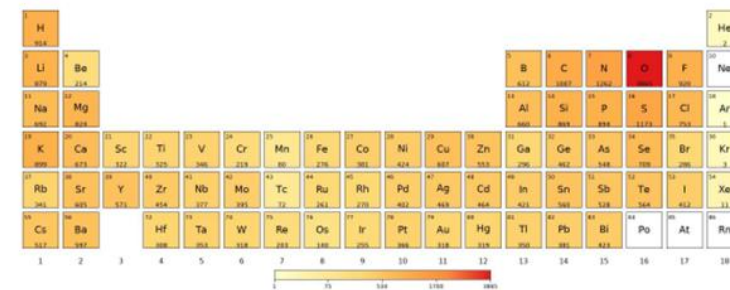
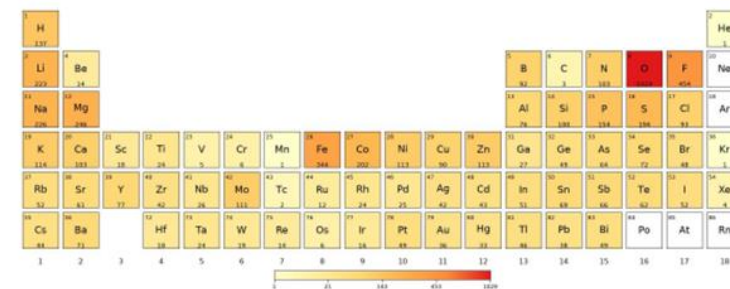


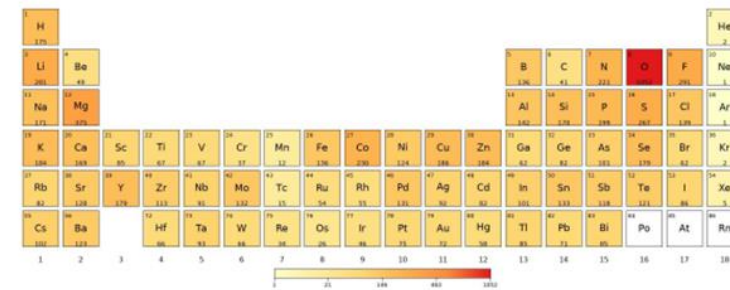
Figure 5: Bar charts of atomic count distributions in the training, validation, and test sets.



(a) Training set



(b) Validation set



(c) Testing set

Figure 6: Statistical charts of element occurrence frequencies in the training, validation, and test sets.

# Results

## Accuracy Performance

- NextHAM demonstrates outstanding generalization across a vast material space spanning >60 elements. It achieves a prediction error of 1.417 meV across R-space Hamiltonian matrices, with errors in the spin-off-diagonal blocks suppressed to the sub- $\mu$ eV scale.
- NextHAM significantly outperforms previous method, e.g., DeepH-E3, in both universal and specialized benchmarks.

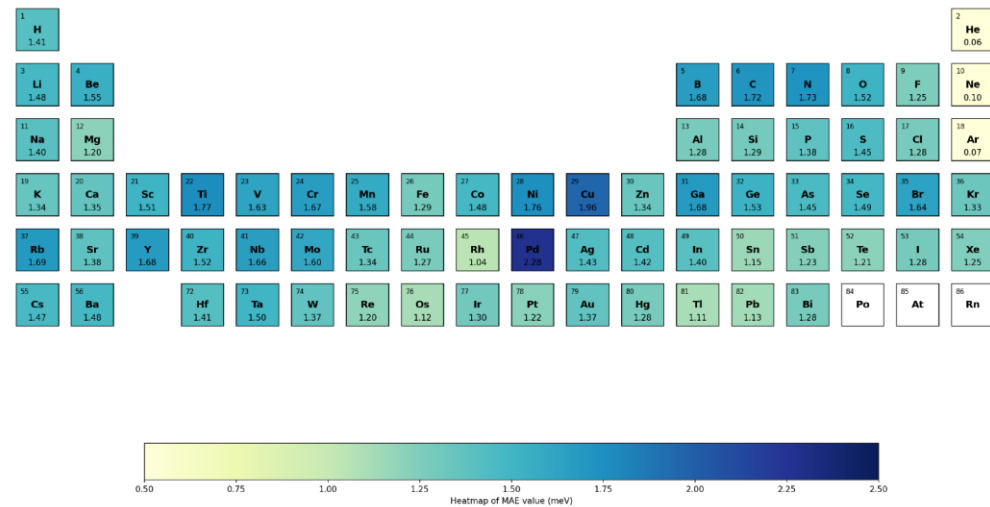


Figure 3: Element-wise analysis of prediction errors. For each chemical element, we collect all of the testing structures containing that element and compute the Gauge MAE values for each subset.

Table 1: Comparison of Gauge MAE values computed in real space (R-space) on the testing set of Materials-HAM-SOC. Values are reported for four spin-resolved regions ( $\uparrow\uparrow$ ,  $\uparrow\downarrow$ ,  $\downarrow\uparrow$ ,  $\downarrow\downarrow$ ) with separate real and imaginary components, and for the entire matrix (Overall), where real and imaginary components are combined into a single metric. Metrics are averaged over non-zero elements only; entries set to zero due to the truncation distance are masked out. All values are in meV.

Region	Gauge_MAE( $\mathbf{0}, \mathbf{H}^{(T)}$ )		Gauge_MAE( $\mathbf{H}^{(0)}, \mathbf{H}^{(T)}$ )		Gauge_MAE( $\mathbf{H}^{(0)} + \widehat{\Delta\mathbf{H}}, \mathbf{H}^{(T)}$ )	
	Real	Imag	Real	Imag	Real	Imag
$\uparrow\uparrow$	149.145	0.293	5.213	< 0.001	2.834	< 0.001
$\uparrow\downarrow$	0.301	0.299	< 0.001	< 0.001	< 0.001	< 0.001
$\downarrow\uparrow$	0.301	0.299	< 0.001	< 0.001	< 0.001	< 0.001
$\downarrow\downarrow$	149.145	0.293	5.213	< 0.001	2.834	< 0.001
Overall	74.914		2.606		<b>1.417</b>	

Table 5: Comparison of R-space errors for DeepH-E3 and our method on the testing set of Materials-HAM-SOC. All values are in meV.

Method	Gauge MAE
DeepH-E3	12.605
<b>Our Method</b>	<b>1.417</b>

Table 7: Comparison of MAE values among DeepH-E3, the original TraceGrad work, and NextHAM<sup>cut-down</sup>. All values are in meV.

Dataset	MAE		
	DeepH-E3	Original TraceGrad	NextHAM <sup>cut-down</sup>
MG	0.251	0.175	<b>0.102</b>
MM	0.406	0.285	<b>0.163</b>

# • Results

## • Efficiency

- The band structures predicted by NextHAM exhibit excellent agreement with the DFT results, effectively suppressing the emergence of “ghost states”.

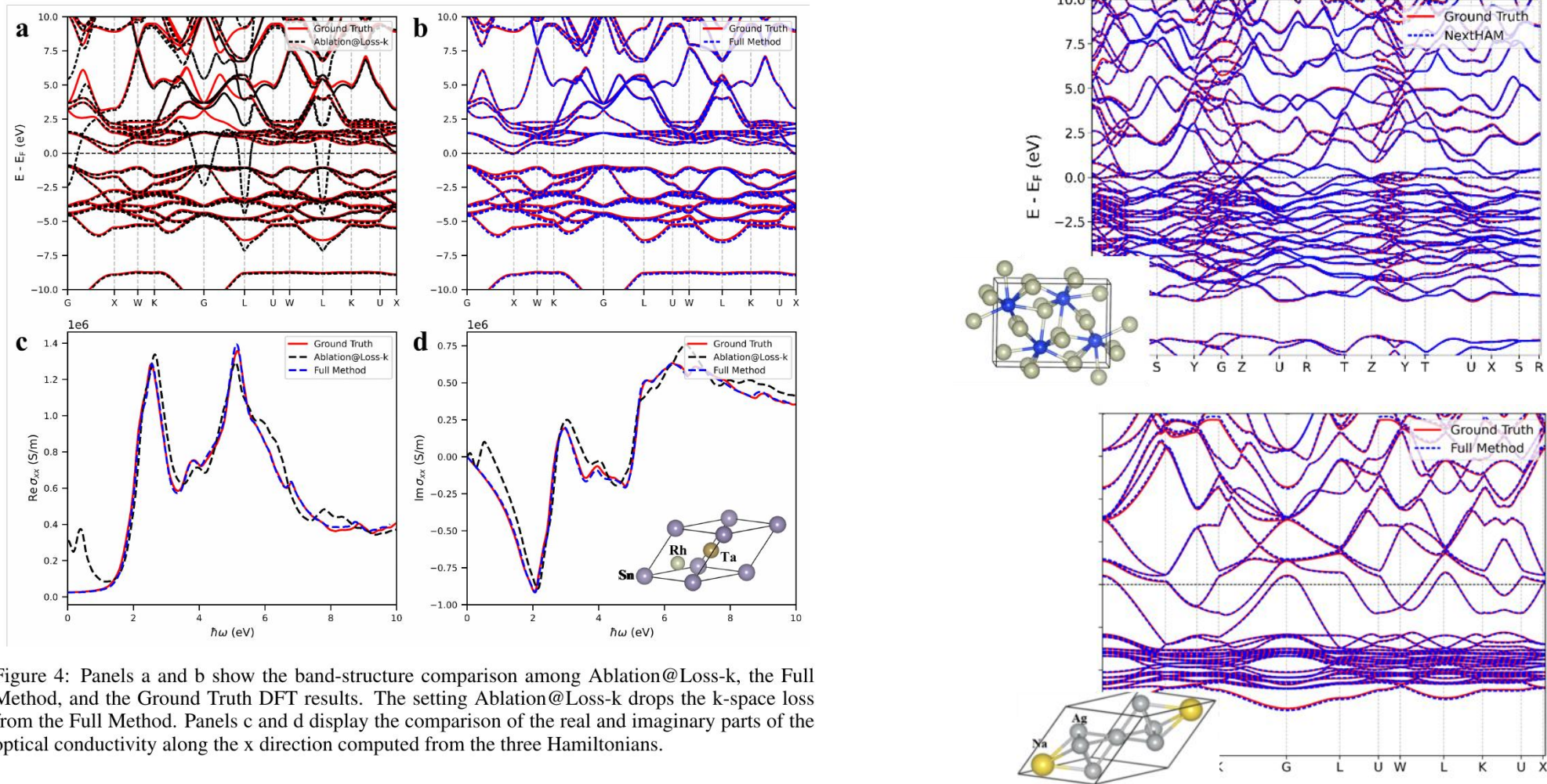


Figure 4: Panels a and b show the band-structure comparison among Ablation@Loss-k, the Full Method, and the Ground Truth DFT results. The setting Ablation@Loss-k drops the k-space loss from the Full Method. Panels c and d display the comparison of the real and imaginary parts of the optical conductivity along the x direction computed from the three Hamiltonians.

# • Results

## • Efficiency

- Comparing to traditional DFT scaling at  $O(TN^3)$  complexity, our method operates at  $O(N^2)$  for small systems and asymptotically approaches linear scaling, at  $O(N)$ , for large systems.
- We have already achieved dramatic empirical speedups on our benchmark dataset. More importantly, because of this  $O(N)$  scaling, the theoretical efficiency potential for ultra-large material systems is even more profound, truly paving the way for large-scale material discovery.

Table 3: Runtime on the testing set of Materials-HAM-SOC (min/max/mean seconds per sample). All stage timings include the data I/O associated with that stage. Note that the total times are computed per sample as the sum of the corresponding stages; therefore their min/max *need not* equal the sum of the per-stage minima/maxima.

Method	Stage	Min (s)	Max (s)	Mean (s)
DFT	$H^{(0)}$ @CPU	3.14	742.43	55.46
	SC@CPU	16.01	28397.45	2251.64
	<b>Total: <math>H^{(0)}</math>@CPU + SC@CPU</b>	21.86	28617.18	2307.11
NextHAM	$H^{(0)}$ @CPU	3.14	742.43	55.46
	NN@CPU	5.15	26.92	12.62
	NN@GPU	1.16	8.95	3.01
	<b>Total: <math>H^{(0)}</math>@CPU + NN@CPU</b>	12.69	755.84	68.08
	<b>Total: <math>H^{(0)}</math>@CPU + NN@GPU</b>	4.84	744.66	58.47